

## Phase stability in high entropy alloys: Formation of solid-solution phase or amorphous phase

Sheng GUO, C. T. LIU

Center of Advanced Structural Materials, MBE Department,  
City University of Hong Kong, Kowloon, Hong Kong, China

Received 21 August 2011; accepted 5 September 2011

**Abstract:** The alloy design for equiatomic multi-component alloys was rationalized by statistically analyzing the atomic size difference, mixing enthalpy, mixing entropy, electronegativity, valence electron concentration among constituent elements in solid solutions forming high entropy alloys and amorphous alloys. Solid solution phases form and only form when the requirements of the atomic size difference, mixing enthalpy and mixing entropy are all met. The most significant difference between the solid solution forming high entropy alloys and bulk metallic glasses lies in the atomic size difference. These rules provide valuable guidance for the future development of high entropy alloys and bulk metallic glasses.

**Key words:** high entropy alloys; amorphous alloys; bulk metallic glasses; phase stability; solid solution

### 1 Introduction

The past twenty years have witnessed the fast development of bulk metallic glasses (BMGs) [1–3], a relatively new type of metallic materials with non-crystalline or amorphous structure. Their unique mechanical and physiochemical properties have stimulated extensive research in the materials community [2–6]. High entropy alloys (HEAs), or equiatomic multi-component alloys that are often in a single solid-solution form, were developed slightly later than the bulk metallic glasses and they even share many similar properties [7–10], but HEAs were given much less attention compared to BMGs. The concept of high-entropy bulk metallic glasses (HE-BMGs) which appeared very recently [11–13] provides an opportunity to compare and study the similarity and difference between these two types of multi-component alloys, particularly, from the alloy design perspective. A critical question relevant to the alloy design for multi-component alloys is: for a given composition with known constituent elements, can we predict which type of phases (amorphous phase, solid solution phase or intermetallic phase) will form? Alternatively, are we now capable of designing the multi-component alloys with the desired phase constitution?

Unfortunately, it is still too ambitious to answer the above two important questions. However, there do have some clues obtained over years of alloy development. For the alloy design of BMGs, the three empirical rules initiated by INOUE [1] have been proven useful: multi-component systems, significant atomic size difference and negative heats of mixing among constituent elements. As traditionally the BMGs have only one or two principle elements, the uncertainty of the suitable composition for other alloying elements complicates the alloy design as there exist too many possibilities to be tried out. It is hence not surprised to see that currently many, if not most, alloy designs for BMGs are based on micro-alloying [14–17] or substitution of similar elements [18, 19] for those mature BMG formers, which were also developed from try-and-error experiments. Along this line of thinking, the alloy design in the equiatomic HEAs could be relatively easier, as once the alloy elements are chosen their compositions are known. However, we now face the uncertainty of the resultant types of crystalline phases: fcc, bcc, mixed fcc and bcc phases [20]. We also know that, in some multi-component alloys with a high mixing entropy (so in principle they can also be called HEAs even they do not form a single solid solution), intermetallics phases can form [20]. As the unique properties of HEAs mostly originate from the formation

of the multi-component solid solution [7, 10], we need to know the rules governing the formation of solid solution phases. Although the name of HEAs and the fact that the HEAs have large mixing entropy give the impression that the mixing entropy is the dominating factor controlling the formation of the solid solution phases, there exists no solid evidence supporting this argument. From the classical Hume-Rothery rule [21] we know that, to form a solid solution, the properties of constituent alloying elements need to be similar: they shall have similar atomic size and similar electronegativity. However, the Hume-Rothery rule is apparently not applicable to the solid solution formation in HEAs. For example, it cannot explain why the equiatomic Co(hcp)-Cr(bcc)-Cu(fcc)-Fe(bcc)-Ni(fcc) alloy forms an fcc-typed solid solution, and how the addition of fcc-Al can eventually change the fcc-type CoCrCuFeNi to a bcc structure [22].

Nevertheless, the prospect of predicting the phase stability from the fundamental properties of the constituent elements is still attractive, and using HEAs as the starting point is ideal in that one can focus on the properties of individual alloying element or their interaction without considering the relative amount of each element. The idea here is to find out the rules governing the phase stability in HEAs by statistically analyzing the collective behavior of the constituent elements in a large database of HEAs, where different phases form, including amorphous phases, solid solution phases or intermetallic phases. ZHANG et al [23] made the first try along this line of thinking, utilizing the atomic size difference, mixing enthalpy and mixing entropy (their definitions will be given in the following section) and some interesting findings were obtained. Solid solution phases are formed when the atomic size difference is small, and the mixing enthalpy is either slightly positive or not very negative; in addition the mixing entropy is high. In contrast, BMGs are formed when the atomic size difference is large, and the mixing enthalpy and mixing entropy are generally more negative and smaller than those of the solid solution forming HEAs. One deficiency of their work is, however, in terms of formation of amorphous phases or solid solution phases, they made the comparison between equiatomic HEAs and non-equiatomic BMGs. As mentioned above, this complicates the analysis by adding the consideration of the relative amount of individual alloying element. In this work, data on amorphous phase forming equiatomic alloy systems are collected and compared with those solid solution forming HEAs, in the hope of finding more trustworthy rules governing the formation of amorphous phase or solid solution phase. It is noted here that the equiatomic alloying systems are not limited to have at least five elements (normally HEAs have at least

five elements), as it is believed by the current authors that the mixing entropy is not the determining factor to form either the solid solution phase or the amorphous phase. This view is also supported by what has been found by ZHANG et al [23].

## 2 Method

In ZHANG et al's work [23], three parameters were used to characterize the collective behavior of the constituent elements in the multi-component alloys: the atomic size difference ( $\delta$ ), the mixing enthalpy ( $\Delta H_{\text{mix}}$ ) and the mixing entropy ( $\Delta S_{\text{mix}}$ ). They were defined by Eqs. (1–3), respectively.

$$\delta = 100 \sqrt{\sum_{i=1}^n c_i (1 - r_i / \bar{r})^2} \quad (1)$$

where  $\bar{r} = \sum_{i=1}^n c_i r_i$ ,  $c_i$  and  $r_i$  are the atomic percentage and atomic radius of the  $i$ th element. The numerical factor 100 was used to amplify the data for clarity; and

$$\Delta H_{\text{mix}} = \sum_{i=1, i \neq j}^n \Omega_{ij} c_i c_j \quad (2)$$

where  $\Omega_{ij} = 4\Delta_{\text{mix}}^{AB}$ ,  $\Delta_{\text{mix}}^{AB}$  is the mixing enthalpy of binary liquid AB alloys; and

$$\Delta S_{\text{mix}} = -R \sum_{i=1}^n c_i \ln c_i \quad (3)$$

where  $R$  is the gas constant.

These three parameters are also adopted in this work. In addition, two more parameters are considered. One is the electronegativity difference,  $\Delta\chi$ , out of consideration from the classical Hume-Rothery's rule to form solid solution phases. It is defined by [24]:

$$\Delta\chi = \sqrt{\sum_{i=1}^n c_i (\chi_i - \bar{\chi})^2} \quad (4)$$

where  $\bar{\chi} = \sum_{i=1}^n c_i \chi_i$ ,  $\chi_i$  is the Pauling electronegativity for the  $i$ th element. The other parameter is the valence electron concentration, VEC, which has been proven useful in determining the phase stability of intermetallic compounds [25, 26]. VEC is defined by:

$$\text{VEC} = \sum_{i=1}^n c_i (\text{VEC})_i \quad (5)$$

where  $(\text{VEC})_i$  is the VEC for the  $i$ th element. It needs to be pointed out here that VEC is different to  $e/a$ , the average number of itinerant electrons per atom in that VEC counts the total electrons including the d-electrons accommodated in the valence band [27, 28]. Except for

the mixing enthalpies of the binary alloys, which can be found in Refs. [29, 30], all the required data for calculation in this work are listed in Table 1 for an easy reference.

### 3 Results

$\Delta H_{\text{mix}}$ ,  $\delta$ ,  $\Delta\chi$ ,  $\Delta S_{\text{mix}}$  and VEC for a series of equiatomic or nearly equiatomic alloys were calculated and are listed in Table 2. When only an amorphous phase forms, the “phase” column in the table shows “amorphous (AM)”; when only solid solution phases form, including different types of solid solutions like mixed fcc and bcc solid solutions, it is marked as “solid

solution (SS)”; once intermetallic phases form (detectable by X-ray diffraction), it is marked as “intermetallics (IM)” in the table. Most of these alloys were prepared by the conventional casting method and the phases we discussed here are hence mostly referring to the as-cast state. It is certainly a concern that these phases are not necessarily in the equilibrium state; however, for many solid solution forming HEAs, it has been shown that the phases formed in the as-cast state are quite stable and hence not far away from the equilibrium state [31–34]. This justifies the motivation to compare their phase stability even at the as-cast state. It is known that the amorphous phase formation depends on the cooling rates and other processing parameters.

**Table 1** Atomic radii, Pauling electronegativity and VEC for elements [46–47]

Element	Symbol	Atomic No.	Radius/Å	Pauling electronegativity	VEC
Lithium	Li	3	1.519	0.98	1
Beryllium	Be	4	1.128	1.57	2
Boron	B	5	0.820	2.04	3
Carbon	C	6	0.773	2.55	4
Nitrogen	N	7	0.750	3.04	5
Oxygen	O	8	0.730	3.44	6
Sodium	Na	11	1.857	0.93	1
Magnesium	Mg	12	1.601	1.31	2
Aluminum	Al	13	1.432	1.61	3
Silicon	Si	14	1.153	1.90	4
Phosphorus	P	15	1.060	2.19	5
Sulfur	S	16	1.020	2.58	6
Potassium	K	19	2.310	0.82	1
Calcium	Ca	20	1.976	1.00	2
Scandium	Sc	21	1.641	1.36	3
Titanium	Ti	22	1.462	1.54	4
Vanadium	V	23	1.316	1.63	5
Chromium	Cr	24	1.249	1.66	6
Manganese	Mn	25	1.350	1.55	7
Iron	Fe	26	1.241	1.83	8
Cobalt	Co	27	1.251	1.88	9
Nickel	Ni	28	1.246	1.91	10
Copper	Cu	29	1.278	1.90	11
Zinc	Zn	30	1.395	1.65	12
Gallium	Ga	31	1.392	1.81	3
Germanium	Ge	32	1.240	2.01	4
Selenium	Se	34	1.400	2.55	6
Rubidium	Rb	37	2.440	0.82	1
Strontium	Sr	38	2.152	0.95	2
Yttrium	Y	39	1.802	1.22	3

(to be continued)

Continue

Element	Symbol	Atomic No.	Radius/Å	Pauling electronegativity	VEC
Zirconium	Zr	40	1.603	1.33	4
Niobium	Nb	41	1.429	1.60	5
Molybdenum	Mo	42	1.363	2.16	6
Technetium	Tc	43	1.360	1.90	7
Ruthenium	Ru	44	1.338	2.20	8
Rhodium	Rh	45	1.345	2.28	9
Palladium	Pd	46	1.375	2.20	10
Silver	Ag	47	1.445	1.93	11
Cadmium	Cd	48	1.568	1.69	12
Indium	In	49	1.659	1.78	3
Tin	Sn	50	1.620	1.96	4
Tellurium	Te	52	1.452	2.10	6
Cesium	Cs	55	2.650	0.79	1
Barium	Ba	56	2.176	0.89	2
Lanthanum	La	57	1.879	1.10	3
Cerium	Ce	58	1.825	1.12	3
Praseodymium	Pr	59	1.650	1.13	3
Neodymium	Nd	60	1.640	1.14	3
Promethium	Pm	61	1.630	1.13	3
Samarium	Sm	62	1.810	1.17	3
Europium	Eu	63	1.984	1.20	3
Gadolinium	Gd	64	1.801	1.20	3
Terbium	Tb	65	1.781	1.10	3
Dysprosium	Dy	66	1.774	1.22	3
Holmium	Ho	67	1.766	1.23	3
Erbium	Er	68	1.756	1.24	3
Thulium	Tm	69	1.560	1.25	3
Ytterbium	Yb	70	1.700	1.10	3
Lutetium	Lu	71	1.735	1.27	3
Hafnium	Hf	72	1.578	1.30	4
Tantalum	Ta	73	1.430	1.50	5
Tungsten	W	74	1.367	2.36	6
Rhenium	Re	75	1.375	1.90	7
Osmium	Os	76	1.352	2.20	8
Iridium	Ir	77	1.357	2.20	9
Platinum	Pt	78	1.387	2.28	10
Gold	Au	79	1.442	2.54	11
Thallium	Tl	81	1.716	1.62	3
Lead	Pb	82	1.750	2.33	4
Polonium	Po	84	1.530	2.00	6
Thorium	Th	90	1.800	1.30	3
Protactinium	Pa	91	1.610	1.50	3
Uranium	U	92	1.420	1.38	3

**Table 2** Calculated parameters  $\Delta H_{\text{mix}}$ ,  $\delta$ ,  $\Delta\chi$ ,  $\Delta S_{\text{mix}}$  and VEC for alloys used in Figs. 1 and 2

Material	VEC	$\Delta\chi$	$\delta$	$\Delta H_{\text{mix}}/(\text{kJ}\cdot\text{mol}^{-1})$	$\Delta S_{\text{mix}}/(\text{J}\cdot\text{K}^{-1}\cdot\text{mol}^{-1})$	Phase	Reference
$\text{Cu}_{0.5}\text{NiAlCoCrFeSi}$	7.00	0.12	6.35	−22.58	16.01	AM	[48]
$\text{Zr}_{17}\text{Ta}_{16}\text{Ti}_{19}\text{Nb}_{22}\text{Si}_{26}$	4.38	0.20	11.08	−48.64	13.25	AM	[49]
$\text{Cu}_{50}\text{Zr}_{50}$	7.50	0.29	11.25	−23.00	5.76	AM	[50]
$\text{Ni}_{50}\text{Nb}_{50}$	7.50	0.16	6.84	−30.00	5.76	AM	[51]
$\text{PdPtCuNiP}$	9.20	0.16	9.29	−23.68	13.38	AM	[13]
$\text{SrCaYbMgZn}$	4.20	0.26	15.25	−13.12	13.38	AM	[12]
$\text{SrCaYbMgZnCu}$	5.33	0.35	18.14	−13.11	14.90	AM	[12]
$\text{SrCaYb}(\text{Li}_{0.55}\text{Mg}_{0.45})\text{Zn}$	4.11	0.26	15.63	−12.15	14.53	AM	[12]
$\text{ErTbDyNiAl}$	4.40	0.30	13.74	−37.60	13.38	AM	[12]
$\text{AlCrTaTiZr}$	4.40	0.11	7.84	−20.00	13.38	AM	[35]
$\text{CuNbNiTiZr}$	6.80	0.22	9.24	−21.28	13.38	AM	[52]
$\text{Zr}_{50}\text{Ti}_{50}$	4.00	0.11	4.57	0.00	5.76	AM	[53]
$\text{Mg}_{50}\text{Cu}_{50}$	6.50	0.30	11.22	−3.00	5.76	AM	[54]
$\text{Zr}_{50}\text{Ni}_{50}$	7.00	0.24	12.50	−49.00	5.76	AM	[53]
$\text{Mg}_{50}\text{Ni}_{50}$	6.00	0.30	12.47	−4.00	5.76	AM	[55]
$\text{ZrHfTiCuNi}$	6.60	0.27	10.32	−27.36	13.38	AM	[56]
$\text{ZrHfTiCuFe}$	6.20	0.25	10.42	−15.84	13.38	AM	[56]
$\text{ZrHfTiCuCo}$	6.40	0.26	10.23	−23.52	13.38	AM	[56]
$\text{Cu}_{0.5}\text{NiAlCoCrFeTi}$	7.00	0.14	6.99	−17.18	16.01	AM	[10]
$\text{Cu}_{0.5}\text{NiAlCoCrFe}$	7.55	0.12	5.51	−7.93	14.70	AM	[10]
$\text{AlCrMoSiTi}$	4.60	0.23	8.68	−34.08	13.38	AM	[57]
$\text{AlCrMoTaTiZr}$	4.67	0.26	9.09	−16.11	14.90	AM	[58]
$\text{AlMoNbSiTaTiVZr}$	4.50	0.24	8.64	−32.19	17.29	AM	[59]
$6\text{FeNiCoSiCrAlTi}$	7.00	0.11	6.56	−21.22	13.21	SS	[60]
$\text{WNbMoTa}$	5.50	0.36	2.31	−6.50	11.53	SS	[61]
$\text{WNbMoTaV}$	5.40	0.34	3.15	−4.64	13.38	SS	[61]
$\text{FeCoNiCrCu}$	8.80	0.09	1.03	3.20	13.38	SS	[22]
$\text{FeCoNiCrCuAl}_{0.3}$	8.47	0.10	3.42	0.16	14.43	SS	[22]
$\text{FeCoNiCrCuAl}_{0.5}$	8.27	0.11	4.17	−1.52	14.70	SS	[22]
$\text{FeCoNiCrCuAl}_{0.8}$	8.00	0.12	4.92	−3.61	14.87	SS	[22]
$\text{FeCoNiCrCuAl}_{1.0}$	7.83	0.12	5.28	−4.78	14.90	SS	[22]
$\text{FeCoNiCrCuAl}_{1.5}$	7.46	0.12	5.89	−7.05	14.78	SS	[22]
$\text{FeCoNiCrCuAl}_{2.0}$	7.14	0.13	6.26	−8.65	14.53	SS	[22]
$\text{FeCoNiCrCuAl}_{2.3}$	6.97	0.13	6.40	−9.38	14.35	SS	[22]
$\text{FeCoNiCrCuAl}_{2.8}$	6.72	0.13	6.57	−10.28	14.01	SS	[22]
$\text{FeCoNiCrCuAl}_3$	6.63	0.13	6.61	−10.56	13.86	SS	[22]
$\text{FeNi}_2\text{CrCuAl}_{0.2}$	8.77	0.10	2.94	0.12	12.01	SS	[20]
$\text{FeNi}_2\text{CrCuAl}_{0.4}$	8.56	0.11	3.86	−1.70	12.45	SS	[20]
$\text{FeNi}_2\text{CrCuAl}_{0.6}$	8.36	0.12	4.49	−3.27	12.72	SS	[20]
$\text{FeNi}_2\text{CrCuAl}_{0.8}$	8.17	0.12	4.96	−4.61	12.88	SS	[20]
$\text{FeNi}_2\text{CrCuAl}_{1.0}$	8.00	0.12	5.32	−5.78	12.98	SS	[20]
$\text{FeNi}_2\text{CrCuAl}_{1.2}$	7.84	0.13	5.60	−6.78	13.02	SS	[20]

(to be continued)

Continue

Material	VEC	$\Delta\chi$	$\delta$	$\Delta H_{\text{mix}}/(\text{kJ}\cdot\text{mol}^{-1})$	$\Delta S_{\text{mix}}/(\text{J}\cdot\text{K}^{-1}\cdot\text{mol}^{-1})$	Phase	Reference
AlCo <sub>0.5</sub> CrCuFeNi	7.73	0.12	5.45	-4.50	14.70	SS	[62]
AlCoCr <sub>0.5</sub> CuFeNi	8.00	0.12	5.44	-5.02	14.70	SS	[62]
AlCoCrCu <sub>0.5</sub> FeNi	7.55	0.12	5.51	-7.93	14.70	SS	[62]
AlCoCrCuFe <sub>0.5</sub> Ni	7.82	0.12	5.40	-5.55	14.70	SS	[62]
AlCoCrCuFeNi <sub>0.5</sub>	7.64	0.12	5.43	-3.90	14.70	SS	[62]
CoCrCu <sub>0.5</sub> FeNi	8.56	0.09	0.84	0.49	13.15	SS	[62]
Al <sub>0.5</sub> CoCrCu <sub>0.5</sub> FeNi	8.00	0.11	4.37	-4.60	14.53	SS	[63]
AlCoCrCu <sub>0.5</sub> FeNi	7.55	0.12	5.51	-7.93	14.70	SS	[63]
Al <sub>1.5</sub> CoCrCu <sub>0.5</sub> FeNi	7.17	0.13	6.12	-10.14	14.53	SS	[63]
Al <sub>2</sub> CoCrCu <sub>0.5</sub> FeNi	6.85	0.13	6.46	-11.60	14.23	SS	[63]
AlCrCu <sub>0.5</sub> FeNi	7.22	0.12	5.92	-7.70	13.15	SS	[63]
AlCo <sub>0.5</sub> CrCu <sub>0.5</sub> FeNi	7.40	0.12	5.71	-7.92	14.53	SS	[63]
AlCoCrCu <sub>0.5</sub> FeNi	7.55	0.12	5.51	-7.93	14.70	SS	[63]
AlCo <sub>1.5</sub> CrCu <sub>0.5</sub> FeNi	7.67	0.12	5.33	-7.83	14.53	SS	[63]
AlCo <sub>2</sub> CrCu <sub>0.5</sub> FeNi	7.77	0.12	5.17	-7.67	14.23	SS	[63]
AlCo <sub>3</sub> CrCu <sub>0.5</sub> FeNi	7.93	0.11	4.88	-7.25	13.48	SS	[63]
AlCo <sub>3.5</sub> CrCu <sub>0.5</sub> FeNi	8.00	0.11	4.75	-7.03	13.09	SS	[63]
AlCoCu <sub>0.5</sub> FeNi	7.89	0.11	5.90	-8.69	13.15	SS	[63]
AlCoCr <sub>0.5</sub> Cu <sub>0.5</sub> FeNi	7.70	0.12	5.70	-8.32	14.53	SS	[63]
AlCoCrCu <sub>0.5</sub> FeNi	7.55	0.12	5.51	-7.93	14.70	SS	[63]
AlCoCr <sub>1.5</sub> Cu <sub>0.5</sub> FeNi	7.42	0.12	5.34	-7.56	14.53	SS	[63]
AlCoCr <sub>2</sub> Cu <sub>0.5</sub> FeNi	7.31	0.12	5.18	-7.20	14.23	SS	[63]
AlCoCrCu <sub>0.5</sub> Ni	7.44	0.13	5.81	-10.17	13.15	SS	[63]
AlCoCrCu <sub>0.5</sub> Fe <sub>0.5</sub> Ni	7.50	0.13	5.66	-8.92	14.53	SS	[63]
AlCoCrCu <sub>0.5</sub> FeNi	7.55	0.12	5.51	-7.93	14.70	SS	[63]
AlCoCrCu <sub>0.5</sub> Fe <sub>1.5</sub> Ni	7.58	0.12	5.37	-7.14	14.53	SS	[63]
AlCoCrCu <sub>0.5</sub> Fe <sub>2</sub> Ni	7.62	0.11	5.23	-6.49	14.23	SS	[63]
AlCoCrCu <sub>0.5</sub> Fe	7.00	0.12	5.87	-6.12	13.15	SS	[63]
AlCoCrCu <sub>0.5</sub> FeNi <sub>0.5</sub>	7.30	0.12	5.68	-7.28	14.53	SS	[63]
AlCoCrCu <sub>0.5</sub> FeNi	7.55	0.12	5.51	-7.93	14.70	SS	[63]
AlCoCrCu <sub>0.5</sub> FeNi <sub>1.5</sub>	7.75	0.12	5.35	-8.28	14.53	SS	[63]
AlCoCrCu <sub>0.5</sub> FeNi <sub>2</sub>	7.92	0.12	5.20	-8.43	14.23	SS	[63]
AlCoCrCu <sub>0.5</sub> FeNi <sub>2.5</sub>	8.07	0.12	5.06	-8.45	13.87	SS	[63]
AlCoCrCu <sub>0.5</sub> FeNi <sub>3</sub>	8.20	0.12	4.93	-8.39	13.48	SS	[63]
CrCuFeMnNi	8.40	0.14	3.20	2.72	13.38	SS	[64]
CoCrFeMnNi	8.00	0.14	3.27	-4.16	13.38	SS	[8]
Al <sub>0.3</sub> CrCuFeMnNi	8.09	0.14	4.21	-0.27	14.43	SS	[64]
Al <sub>0.5</sub> CrCuFeMnNi	7.91	0.14	4.66	-1.92	14.70	SS	[64]
Al <sub>0.8</sub> CrCuFeMnNi	7.66	0.14	5.15	-3.97	14.87	SS	[64]
AlCrCuFeMnNi	7.50	0.14	5.39	-5.11	14.90	SS	[64]
Al <sub>0.8</sub> CrCu <sub>1.5</sub> FeMnNi	7.92	0.14	4.96	-1.74	14.74	SS	[64]
Al <sub>0.8</sub> CrCuFe <sub>1.5</sub> MnNi	7.68	0.14	5.08	-3.31	14.74	SS	[64]
Al <sub>0.8</sub> CrCuFeMn <sub>1.5</sub> Ni	7.60	0.15	5.05	-4.23	14.74	SS	[64]

(to be continued)

Continue

Material	VEC	$\Delta\chi$	$\delta$	$\Delta H_{\text{mix}}/(\text{kJ}\cdot\text{mol}^{-1})$	$\Delta S_{\text{mix}}/(\text{J}\cdot\text{K}^{-1}\cdot\text{mol}^{-1})$	Phase	Reference
CuAlNiCoCrFeSi	7.29	0.12	6.13	−18.86	16.18	SS	[65]
AlCoCrCuFeMoNiTiVZr	6.60	0.22	8.54	−17.24	19.14	SS	[66]
CoCrFeNiTi	7.40	0.14	6.68	−16.32	13.38	IM	[52]
NbCrFeMnCoNi	7.50	0.14	5.49	−12.00	14.90	IM	[8]
TiCrFeMnCoNi	7.33	0.15	6.29	−13.44	14.90	IM	[8]
TiVCrCuFeMnCoNi	7.50	0.15	5.50	−8.13	17.29	IM	[67]
Ti <sub>2</sub> CrCuFeCoNi	7.43	0.15	7.24	−14.04	14.53	IM	[23]
AlTiVYZr	3.80	0.16	10.95	−14.88	13.38	IM	[23]
ZrTiVCuNiBe	6.00	0.20	11.48	−24.89	14.90	IM	[23]
CoCrCuFeNiTi <sub>0.8</sub>	8.14	0.13	5.70	−6.75	14.87	IM	[68]
CoCrCuFeNiTi <sub>1.0</sub>	8.00	0.14	6.12	−8.44	14.90	IM	[68]
Al <sub>0.5</sub> CoCrCuFeNiTi <sub>0.8</sub>	7.73	0.14	6.26	−10.11	16.00	IM	[69]
Al <sub>0.5</sub> CoCrCuFeNiTi <sub>1.0</sub>	7.62	0.14	6.54	−11.60	16.01	IM	[69]
Al <sub>0.5</sub> CoCrCuFeNiTi <sub>1.2</sub>	7.51	0.14	6.76	−12.89	15.97	IM	[69]
Al <sub>0.5</sub> CoCrCuFeNiTi <sub>1.4</sub>	7.41	0.15	6.94	−14.02	15.91	IM	[69]
Al <sub>0.5</sub> CoCrCuFeNiTi <sub>1.6</sub>	7.31	0.15	7.09	−15.01	15.82	IM	[69]
Al <sub>0.5</sub> CoCrCuFeNiTi <sub>1.8</sub>	7.22	0.15	7.21	−15.86	15.72	IM	[69]
Al <sub>0.5</sub> CoCrCuFeNiTi <sub>2.0</sub>	7.13	0.15	7.31	−16.60	15.60	IM	[69]
Al <sub>0.5</sub> CoCrCuFeNiV <sub>0.6</sub>	7.95	0.12	4.09	−4.07	15.92	IM	[70]
Al <sub>0.5</sub> CoCrCuFeNiV <sub>0.8</sub>	7.86	0.12	4.07	−4.71	16.00	IM	[70]
Al <sub>0.5</sub> CoCrCuFeNiV <sub>1.0</sub>	7.77	0.12	4.04	−5.25	16.01	IM	[70]
ZrHfTiAlCuNi	6.00	0.24	9.42	−34.11	14.90	IM	[71]
AlCoCrFeNiTi <sub>1.5</sub>	6.46	0.15	7.50	−23.91	14.78	IM	[72]
Zr <sub>41.2</sub> Ti <sub>13.8</sub> Cu <sub>12.5</sub> Ni <sub>10</sub> Be <sub>22.5</sub>	5.03	0.22	13.96	−35.20	12.18	AM	[38]
Pd <sub>40</sub> Cu <sub>30</sub> Ni <sub>10</sub> P <sub>20</sub>	9.30	0.14	9.08	−24.88	10.64	AM	[38]
Fe <sub>41</sub> Co <sub>7</sub> Cr <sub>15</sub> Mo <sub>14</sub> C <sub>15</sub> B <sub>6</sub> Y <sub>2</sub>	6.49	0.30	18.56	−33.35	13.66	AM	[38]
Mg <sub>54</sub> Cu <sub>26.5</sub> Ag <sub>8.5</sub> Gd <sub>11</sub>	5.26	0.30	11.02	−8.45	9.45	AM	[38]
Cu <sub>46</sub> Zr <sub>42</sub> Al <sub>7</sub> Y <sub>5</sub>	7.10	0.28	11.84	−24.88	8.79	AM	[38]
Y <sub>36</sub> Sc <sub>20</sub> Al <sub>24</sub> Co <sub>20</sub>	4.20	0.25	13.55	−34.92	11.26	AM	[38]
Co <sub>48</sub> Cr <sub>15</sub> Mo <sub>14</sub> C <sub>15</sub> B <sub>6</sub> Er <sub>2</sub>	6.90	0.29	18.40	−33.36	12.00	AM	[38]
Ti <sub>40</sub> Zr <sub>25</sub> Cu <sub>12</sub> Ni <sub>3</sub> Be <sub>20</sub>	6.54	0.20	16.72	−25.88	11.59	AM	[38]
Pt <sub>42.5</sub> Cu <sub>27</sub> Ni <sub>9.5</sub> P <sub>21</sub>	9.22	0.17	9.64	−24.94	10.55	AM	[38]
Ca <sub>65</sub> Mg <sub>15</sub> Zn <sub>20</sub>	4.00	0.26	13.47	−14.26	7.37	AM	[38]

AM stands for amorphous phases, SS for solid solution phases and IM for intermetallic phases

However, in this analysis, as long as a single amorphous phase can be achieved via ordinary preparation processes, the alloys are identified as the amorphous phase forming alloys in the table. For example, when rods of diameter smaller than 10 mm are cast, the equiatomic PdPtCuNiP alloy has a single amorphous structure but crystalline phases form at larger sizes [13]. PdPtCuNiP is identified as the amorphous phase forming alloy in Table 2. Another example is, when in the bulk as-cast form, the phases in the

equiatomic AlCrTaTiZr comprise a bcc solid solution plus an Al<sub>2</sub>Zr compound; however, when it was deposited into thin film by the RF magnetron sputtering, a single amorphous phase was obtained [35]. AlCrTaTiZr is also identified as the amorphous phase forming alloy in Table 2. Then a question naturally arises: would those solid solution forming alloys form amorphous phases when they are deposited into films? To the knowledge of the current authors, there is no reported work on this topic. On one hand, in principle any alloy even pure

metal can become amorphous if sufficiently high cooling rate is given when it cools from the liquid state [36], so this is actually not a critical question; on the other hand, available data show that some equiatomic alloys cannot form amorphous phases and instead they form solid solution phases using the sputtering method [37]. It suggests that the fundamental properties of constituent alloying elements do make a difference on forming the solid solution phase or amorphous phase at comparable preparation conditions. This justifies the classification of formed phases in Table 2. For the purpose of comparison,  $\Delta H_{\text{mix}}$ ,  $\delta$ ,  $\Delta\chi$ ,  $\Delta S_{\text{mix}}$  and VEC for some non-equiatomic BMGs with good glass forming ability (GFA) [38] were

also calculated and are listed in the bottom of Table 2.

For clarity, the data in Table 2 are plotted in Fig. 1, to show how the five parameters reflecting the collective behavior of the constituent alloying elements, can affect the phase stability in HEAs, particularly to reveal the rules governing the formation of solid solution phases and amorphous phases. From Fig. 1, we can see that solid solution phases form when  $\Delta H_{\text{mix}}$  is slightly positive or not very negative and when  $\delta$  is small, and  $\Delta S_{\text{mix}}$  is high. Comparatively, amorphous phases generally form at more negative  $\Delta H_{\text{mix}}$ , larger  $\delta$  and smaller  $\Delta S_{\text{mix}}$ , no matter in equiatomic or non-equiatomic alloys. This is basically in agreement to the findings by

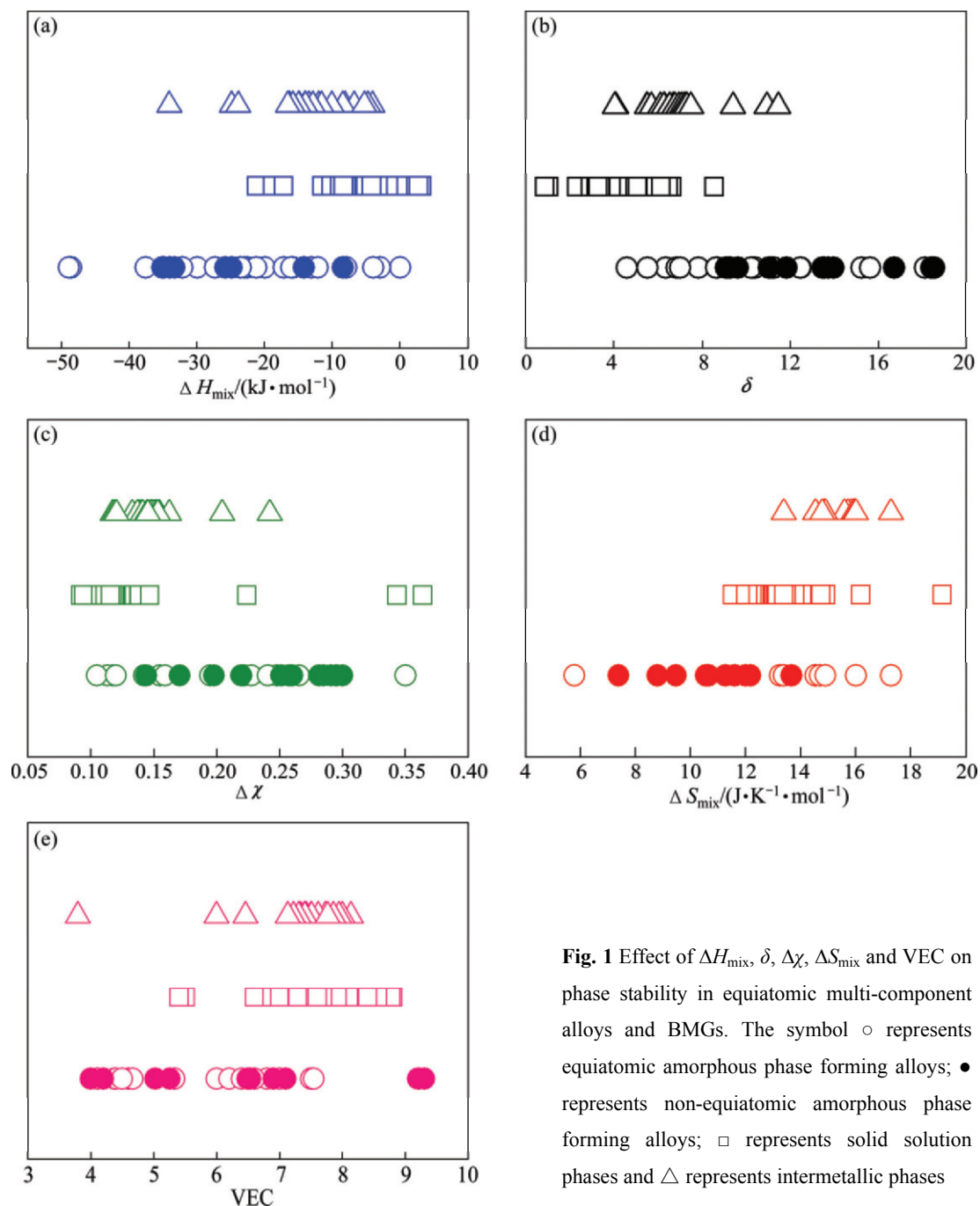


**Fig. 1** Effect of  $\Delta H_{\text{mix}}$ ,  $\delta$ ,  $\Delta\chi$ ,  $\Delta S_{\text{mix}}$  and VEC on phase stability in equiatomic multi-component alloys and BMGs. The symbol ○ represents equiatomic amorphous phase forming alloys; ● represents non-equiatomic amorphous phase forming alloys; □ represents solid solution phases and △ represents intermetallic phases



ZHANG et al [23], but the difference here is that we added the data for the equiatomic amorphous phase forming alloys. As we mentioned before, this ensures the phase stability analysis is compared simply from the fundamental properties of the constituent elements, and not from their relative amount.  $\Delta\chi$  almost does not have an effect on the formation of solid solution phase or amorphous phase. VEC also has a weak effect on the phase stability between the amorphous phases and solid solution phases. It is important to note that, in a previous work [20], we have shown that VEC plays a decisive role in determining the fcc- or bcc-type solid solution in HEAs, and specially larger  $VEC(\geq 8)$  favors the formation of fcc-type solid solutions, while smaller  $VEC(<6.87)$  favors the formation of bcc-type solid solutions.

To better reflect the three main factors governing the phase stability,  $\Delta H_{\text{mix}}$ ,  $\delta$ , and  $\Delta S_{\text{mix}}$  are superimposed, as shown in Fig. 2. It clearly shows that solid solution phases form and only form when the three parameters,  $\Delta H_{\text{mix}}$ ,  $\delta$ , and  $\Delta S_{\text{mix}}$  are in the suitable range:  $0 \leq \delta \leq 8.5$ ,  $-22 \leq \Delta H_{\text{mix}} \leq 7$  kJ/mol and  $11 \leq \Delta S_{\text{mix}} \leq 19.5$  J/(K·mol). The restrictions for forming amorphous phases from these three parameters are much relaxed, as can be seen from the distribution of the data points. However, the region where BMGs form is limited:  $\delta \geq 9$ ,  $-35 \leq \Delta H_{\text{mix}} \leq -8.5$  kJ/mol and  $7 \leq \Delta S_{\text{mix}} \leq 14$  J/(K·mol). The range for forming BMGs could be larger as only some excellent glass formers are included here. This will be discussed further in the following section. It is surprised to note how the atomic size difference,  $\delta$ , can separate the formation of solid solution phases and the BMGs. Interestingly, intermetallic phases tend to form at the intermediate conditions in terms of these three parameters, particular for  $\delta$ . In the region where solid solution phases form, intermetallic phases can also form while only a few marginal glass formers are found. Seen from Fig. 2(c), it suggests that by decreasing  $\delta$  to roughly  $\delta < 4$  while keeping  $\Delta H_{\text{mix}}$  and  $\Delta S_{\text{mix}}$  falling in the solid solution forming region, only solid solution phases would form.

## 4 Discussion

### 4.1 Indications on solid solution phase formation

From Fig. 2, it is immediately obvious that only satisfying the high mixing entropy requirement is not sufficient to form solid solution phases in equiatomic multi-component alloys, as is felt from the name of high entropy alloys. The mixing entropy reflects the complexity of the system, and the higher mixing entropy the more confused the system gets to form ordered structure [39]. From this perspective, the formation of random solid solution or partially ordered solid solution is favored by the high mixing entropy. However, another

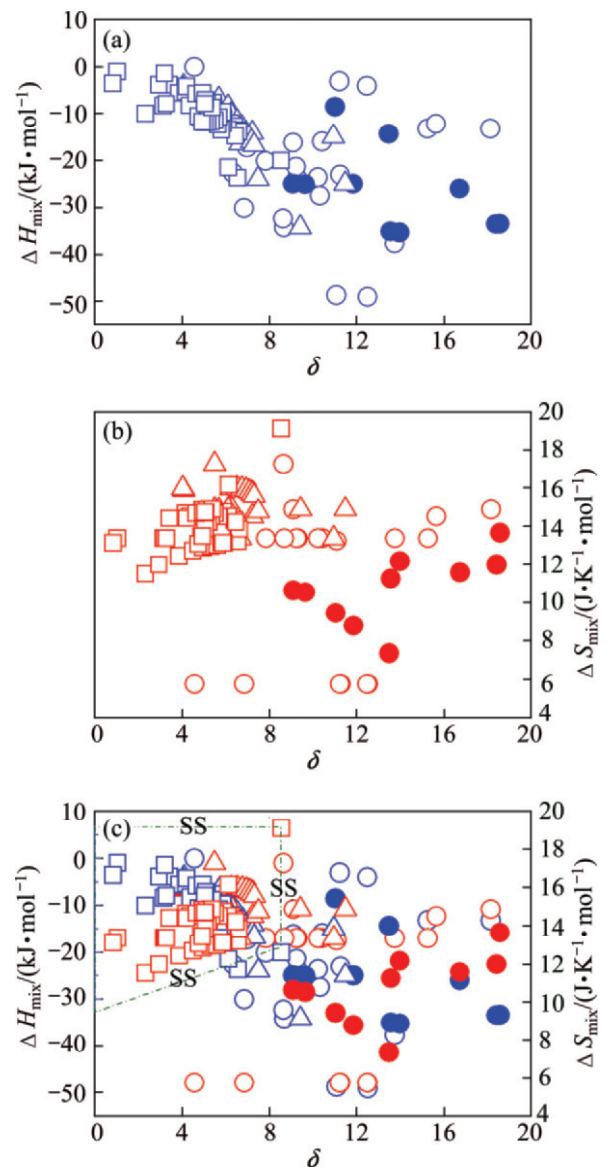


**Fig. 2** Superimposed effect of  $\Delta H_{\text{mix}}$  and  $\delta$  (a),  $\Delta S_{\text{mix}}$  and  $\delta$  (b), and all three parameters  $\Delta H_{\text{mix}}$ ,  $\delta$  and  $\Delta S_{\text{mix}}$  (c) on phase stability in equiatomic multi-component alloys and BMGs. The symbol  $\circ$  represents equiatomic amorphous phase forming alloys;  $\bullet$  represents non-equiatomic amorphous phase forming alloys;  $\square$  represents solid solution phases and  $\triangle$  represents intermetallic phases. The region delineated by the dash-dotted lines in (c) indicates the requirements for solid solution phases to form.

possibility when the system gets confused is to form the amorphous phase. Naturally, the amorphous phase formation needs to be inhibited to form the solid solution phases, and here come the other requirements such as atomic size difference and mixing enthalpy. The requirement on the small size difference can be perceived by the notion of topological instability proposed by EGAMI [40–42]. Atoms suffer from pressure under the atomic size mismatch and this produces the local elastic

strain. Above some critical volume strain the system becomes topological unstable and glass transition might happen. The requirement on the mixing enthalpy could be related to the cluster formation in that the more negative mixing enthalpy favors the formation of chemically ordered clusters that are related to the high GFA [43–45], hence not favors the formation of the solid solution. To form stable glassy phase, however, the more negative enthalpy has to be coupled with the large atomic size difference, otherwise intermetallic phases would form. This will be discussed further in the coming section.

#### 4.2 Indication on non-equiatomic BMGs formation

As this paper mainly addresses to the phase competition between solid solution phases and amorphous phases in multi-component alloys, it is certainly relevant to discuss the indication of the collective behavior of constituent alloying elements on the BMG formation, which is another important and unsettled topic. In Fig. 3, the effect of  $\Delta H_{\text{mix}}$ ,  $\delta$ , and  $\Delta S_{\text{mix}}$  on the critical cooling rates ( $R_c$ ) for the non-equiatomic metallic glasses with a broad range of GFA is plotted. The relevant parameters used in Fig. 3 are given in Table 3. Although  $\delta$  plays a decisive role in determining the formation of solid solution or BMGs, it does not have a direct impact on the GFA seen from Fig. 3(a). If we assume those metallic glasses with  $R_c \leq 10^2$  K/s can be considered as in the bulk form, it is interesting to note that BMGs all have  $\delta \geq 9$ , which is in agreement with the observation from Fig. 1(b) and Fig. 2.  $\Delta H_{\text{mix}}$  also has a weak correlation to  $R_c$ , although generally BMGs have more negative  $\Delta H_{\text{mix}}$  and the range for forming BMGs is  $-40 \leq \Delta H_{\text{mix}} \leq -5.5$  kJ/mol, which is broader than that obtained from Fig. 1(a) and Fig. 2, as more alloy systems are reflected in Fig. 3(b). Different to  $\delta$  and  $\Delta H_{\text{mix}}$ ,  $\Delta S_{\text{mix}}$  apparently has a reasonable correlation to  $R_c$ , and the higher  $\Delta S_{\text{mix}}$  the lower  $R_c$ . All BMGs with good GFA have  $\Delta S_{\text{mix}} \geq 7$  J/(K·mol) and again this agrees to the conclusion obtained from Fig. 1(d) and Fig. 2. This actually justifies the requirement for multiple alloying elements for forming BMGs, and basically the conclusions from Fig. 3 are all consistent with INOUE's three empirical rules [1].

#### 4.3 Indication on HE-BMGs formation

The emergence of HE-BMGs or equiatomic BMGs [11–13] is exciting as this would greatly simplify the alloy design and it also provides a brand new perspective to develop BMGs, different to the traditional alloy design for BMGs that are based on one or two principle elements. Essentially, those parameters favoring the formation of BMGs shall also favor the formation of

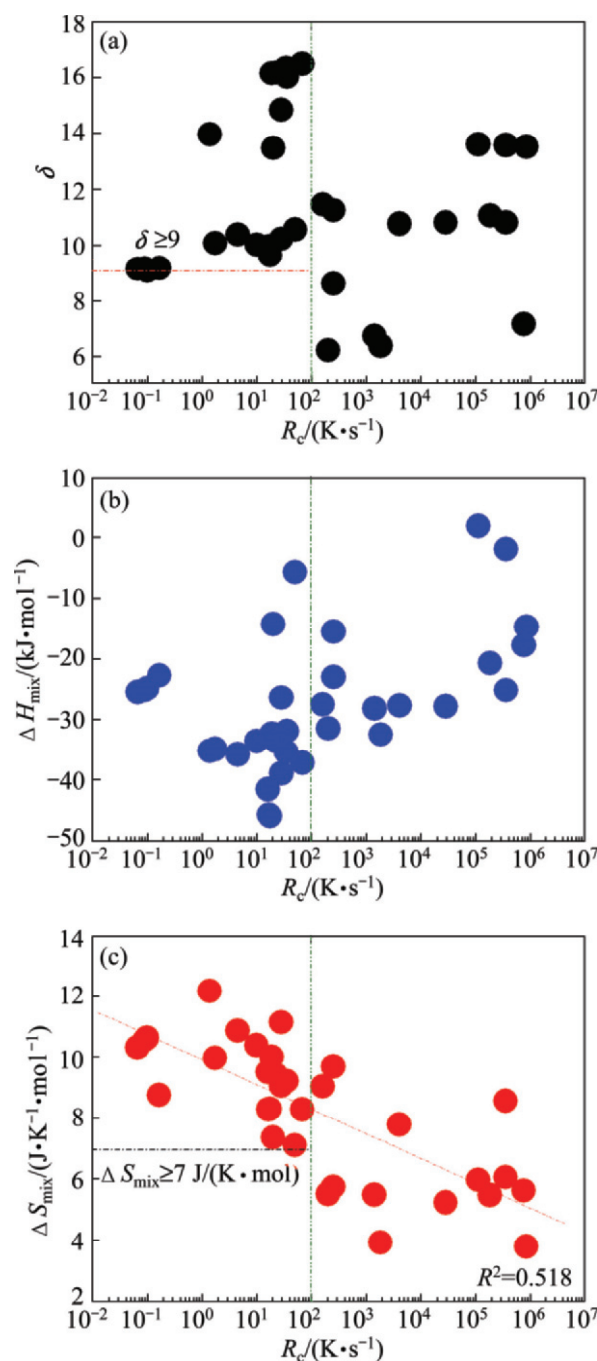


**Fig. 3** Effect of  $\delta$  (a),  $\Delta H_{\text{mix}}$  (b) and  $\Delta S_{\text{mix}}$  (c) on critical cooling rates for metallic glasses

HE-BMGs. This is verified in Fig. 4, where  $\Delta H_{\text{mix}}$ ,  $\delta$ , and  $\Delta S_{\text{mix}}$  for the equiatomic amorphous phase forming alloys are plotted separately and those BMG formers (with size larger than 1 mm) are represented by the closed-circle symbols for clarity. It is clear that the equiatomic or high-entropy BMGs form when  $\delta \geq 9$ ,  $-49 \leq \Delta H_{\text{mix}} \leq -5.5$  kJ/mol and  $7 \leq \Delta S_{\text{mix}} \leq 16$  J/(K·mol) (indicated by the green dash-dotted line in Fig. 4(c)), at almost the exact region where non-equiatomic BMGs form. A closer look at Fig. 4(c) suggests that most

**Table 3** Critical cooling rates  $R_c$ , and  $\delta$ ,  $\Delta H_{\text{mix}}$ ,  $\Delta S_{\text{mix}}$  for alloys used in Fig. 3 ( $R_c$  data from Ref. [73] and references wherein)

Material	$R_c$	$\delta$	$\Delta H_{\text{mix}}/(\text{kJ}\cdot\text{mol}^{-1})$	$\Delta S_{\text{mix}}/(\text{J}\cdot\text{K}^{-1}\cdot\text{mol}^{-1})$
La <sub>55</sub> Al <sub>25</sub> Ni <sub>20</sub>	$6.75\times 10^1$	16.50	-37.18	8.29
La <sub>55</sub> Al <sub>25</sub> Ni <sub>15</sub> Cu <sub>5</sub>	$3.45\times 10^1$	16.35	-35.35	9.23
La <sub>55</sub> Al <sub>25</sub> Ni <sub>10</sub> Cu <sub>10</sub>	$2.25\times 10^1$	16.19	-33.60	9.44
La <sub>55</sub> Al <sub>25</sub> Ni <sub>5</sub> Cu <sub>15</sub>	$3.59\times 10^1$	16.04	-31.93	9.23
La <sub>55</sub> Al <sub>25</sub> Ni <sub>5</sub> Cu <sub>10</sub> Co <sub>5</sub>	$1.88\times 10^1$	16.17	-32.31	10.02
Pd <sub>40</sub> Ni <sub>40</sub> P <sub>20</sub>	$1.67\times 10^{-1}$	9.17	-22.72	8.77
Pd <sub>40</sub> Ni <sub>10</sub> Cu <sub>30</sub> P <sub>20</sub>	$1.00\times 10^{-1}$	9.08	-24.88	10.64
Pd <sub>42.5</sub> Cu <sub>30</sub> Ni <sub>7.5</sub> P <sub>20</sub>	$6.70\times 10^{-2}$	9.15	-25.46	10.32
Pd <sub>43</sub> Cu <sub>27</sub> Ni <sub>10</sub> P <sub>20</sub>	$9.00\times 10^{-2}$	9.17	-25.17	10.55
Pd <sub>77.5</sub> Cu <sub>6</sub> Si <sub>16.5</sub>	$2.00\times 10^2$	6.23	-31.49	5.52
Pd <sub>82</sub> Si <sub>18</sub>	$1.80\times 10^3$	6.39	-32.47	3.92
Zr <sub>41.2</sub> Ti <sub>13.8</sub> Cu <sub>12.5</sub> Ni <sub>10</sub> Be <sub>22.5</sub>	$1.40\times 10^0$	13.96	-35.20	12.18
Zr <sub>46.75</sub> Ti <sub>8.25</sub> Cu <sub>7.5</sub> Ni <sub>10</sub> Be <sub>27.5</sub>	$2.80\times 10^1$	14.85	-38.92	11.15
Zr <sub>52.5</sub> Cu <sub>17.9</sub> Ni <sub>14.6</sub> Al <sub>10</sub> Ti <sub>5</sub>	$4.50\times 10^0$	10.38	-35.79	10.87
Zr <sub>55</sub> Al <sub>19</sub> Co <sub>19</sub> Cu <sub>7</sub>	$1.60\times 10^1$	9.89	-41.55	9.53
Zr <sub>55</sub> Al <sub>20</sub> Co <sub>25</sub>	$1.65\times 10^1$	9.96	-45.71	8.29
Zr <sub>55</sub> Al <sub>22.5</sub> Co <sub>22.5</sub>	$1.75\times 10^1$	9.64	-45.92	8.31
Zr <sub>57</sub> Cu <sub>15.4</sub> Ni <sub>12.6</sub> Al <sub>10</sub> Nb <sub>5</sub>	$1.00\times 10^1$	10.02	-33.61	10.39
Zr <sub>58.5</sub> Cu <sub>15.6</sub> Ni <sub>12.8</sub> Al <sub>10.3</sub> Nb <sub>2.8</sub>	$1.75\times 10^0$	10.08	-34.91	9.98
Mg <sub>65</sub> Cu <sub>25</sub> Y <sub>10</sub>	$5.00\times 10^1$	10.56	-5.71	7.12
Cu <sub>47</sub> Ti <sub>34</sub> Zr <sub>11</sub> Ni <sub>8</sub>	$2.50\times 10^2$	8.61	-15.44	9.70
Cu <sub>50</sub> Zr <sub>50</sub>	$2.50\times 10^2$	11.25	-23.00	5.76
Fe <sub>41.5</sub> Ni <sub>41.5</sub> B <sub>17</sub>	$3.50\times 10^5$	13.58	-1.94	8.57
Fe <sub>79</sub> Si <sub>10</sub> B <sub>11</sub>	$1.80\times 10^5$	11.07	-20.71	5.48
Fe <sub>80</sub> P <sub>13</sub> C <sub>7</sub>	$2.80\times 10^4$	10.82	-27.80	5.24
Fe <sub>83</sub> B <sub>17</sub>	$8.30\times 10^5$	13.52	-14.67	3.79
Ni <sub>62.4</sub> Nb <sub>37.6</sub>	$1.40\times 10^3$	6.74	-28.16	5.50
Ni <sub>75</sub> Si <sub>8</sub> B <sub>17</sub>	$1.10\times 10^5$	13.60	1.88	5.98
Co <sub>75</sub> Si <sub>15</sub> B <sub>10</sub>	$3.50\times 10^5$	10.82	-25.14	6.07
Au <sub>77.8</sub> Ge <sub>13.8</sub> Si <sub>8.4</sub>	$7.40\times 10^5$	7.17	-17.75	5.63
Pt <sub>57.5</sub> Cu <sub>14.7</sub> Ni <sub>5.3</sub> P <sub>22.5</sub>	$2.80\times 10^1$	10.24	-26.36	9.07
Pt <sub>60</sub> Ni <sub>15</sub> P <sub>25</sub>	$4.00\times 10^3$	10.77	-27.68	7.80
Pr <sub>60</sub> Cu <sub>20</sub> Ni <sub>10</sub> Al <sub>10</sub>	$1.60\times 10^2$	11.46	-27.52	9.05
Ca <sub>65</sub> Mg <sub>15</sub> Zn <sub>20</sub>	$2.00\times 10^1$	13.47	-14.26	7.37

HE-BMGs form at a much narrower region indicated by the blue dash-dotted line in Fig. 4(c):  $\delta \geq 9$ ,  $-28 \leq \Delta H_{\text{mix}} \leq -10$  kJ/mol and  $13.38 \leq \Delta S_{\text{mix}} \leq 14.89$  J/(K·mol). The mixing entropies of 13.38 and 14.89 J/(K·mol) correspond to the mixing entropy for the equiatomic and quinary and senary alloys. This refined

region could provide a guideline to find more HE-BMGs. Although there lack sufficient information to establish correlations between the critical cooling rates and the parameters like  $\Delta H_{\text{mix}}$ ,  $\delta$ , or  $\Delta S_{\text{mix}}$  for HE-BMGs, the fact that most HE-BMGs fall in the high  $\Delta S_{\text{mix}}$  region suggests that the high mixing entropy favors BMG

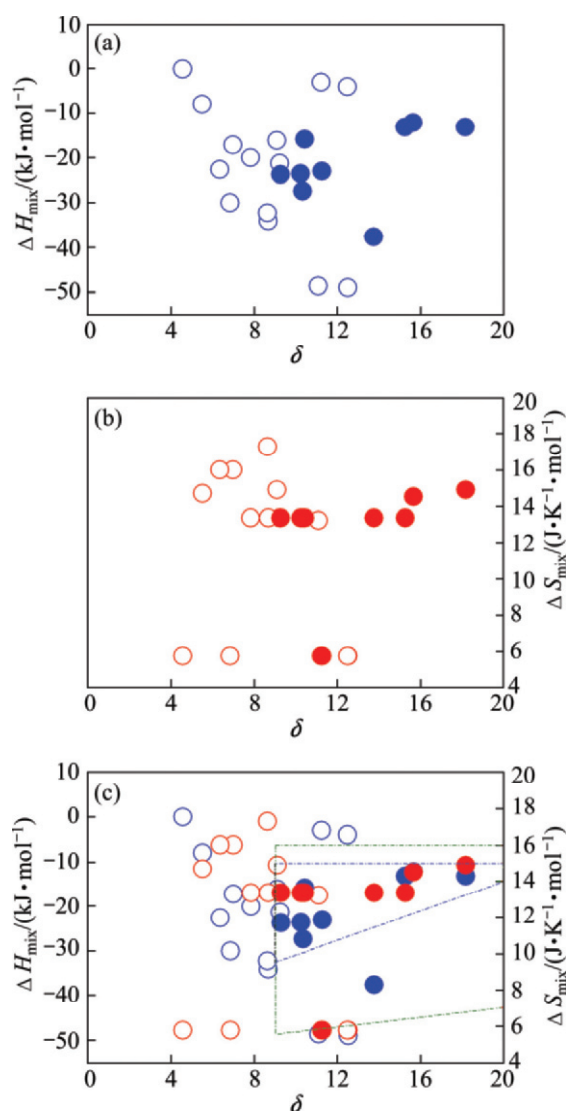


**Fig. 4** Superimposed effect of  $\Delta H_{\text{mix}}$  and  $\delta$  (a),  $\Delta S_{\text{mix}}$  and  $\delta$  (b), and all three parameters  $\Delta H_{\text{mix}}$ ,  $\delta$ ,  $\Delta S_{\text{mix}}$  (c) on phase stability in equiatomic multi-component amorphous alloys. The symbols  $\circ$  represent marginal glass formers and  $\bullet$  represent bulk glass formers. The region delineated by the dash-dotted lines in (c) indicates the requirements for BMG formation

formation, in consistent to the conclusion obtained from non-equiatomic BMGs (Fig. 3(c)).

## 5 Conclusions

1) The high mixing entropy is not the only factor that controls the solid solution formation in equiatomic multi-component alloys. The formation of solid solution requires that the mixing enthalpy ( $\Delta H_{\text{mix}}$ ), atomic size difference ( $\delta$ ) and mixing entropy simultaneously satisfy  $-22 \leq \Delta H_{\text{mix}} \leq 7$  kJ/mol,  $0 \leq \Delta S_{\text{mix}} \leq 8.5$ , and  $11 \leq \Delta S_{\text{mix}} \leq 19.5$  J/(K·mol).

2) The atomic size difference is the critical parameter that determines the formation of solid solution

phases or bulk metallic glasses. BMGs form when  $\delta \geq 9$ ,  $-49 \leq \Delta H_{\text{mix}} \leq -5.5$  kJ/mol and  $7 \leq \Delta S_{\text{mix}} \leq 16$  J/(K·mol), for both equiatomic and non-equiatomic alloys.

3) In terms of the glass forming ability, the high mixing entropy favors the formation of BMGs.

## Acknowledgements

This research was supported by the Initial Funding from CityU.

## References

- [1] INOUE A. Stabilization of metallic supercooled liquid and bulk amorphous alloys [J]. *Acta Materialia*, 2000, 48: 279–306.
- [2] JOHNSON W L. Bulk glass-forming metallic alloys: Science and technology [J]. *MRS Bulletin*, 1999, 24: 42–56.
- [3] WANG W H, DONG C, SHEK C H. Bulk metallic glasses [J]. *Materials Science & Engineering R-Reports*, 2004, 44: 45–89.
- [4] SCHUH C A, HUFNAGEL T C, RAMAMURTY U. Mechanical behavior of amorphous alloys [J]. *Acta Materialia*, 2007, 55: 4067–4109.
- [5] ASHBY M F, GREER A L. Metallic glasses as structural materials [J]. *Scripta Materialia*, 2006, 54: 321–326.
- [6] LOFFLER J F. Bulk metallic glasses [J]. *Intermetallics*, 2003, 11: 529–540.
- [7] YEH J W, CHEN S K, LIN S J, et al. Nanostructured high-entropy alloys with multiple principal elements: Novel alloy design concepts and outcomes [J]. *Advanced Engineering Materials*, 2004, 6: 299–303.
- [8] CANTOR B, CHANG I T H, KNIGHT P, et al. Microstructural development in equiatomic multicomponent alloys [J]. *Materials Science and Engineering A*, 2004, 375–377: 213–218.
- [9] WU W H, YANG C C, YEH J W. Industrial development of high-entropy alloys [J]. *Annales De Chimie-Science Des Materiaux*, 2006, 31: 737–747.
- [10] YEH J W. Recent progress in high-entropy alloys [J]. *Annales De Chimie-Science Des Materiaux*, 2006, 31: 633–648.
- [11] ZHAO K, XIA X X, BAI H Y, et al. Room temperature homogeneous flow in a bulk metallic glass with low glass transition temperature [J]. *Applied Physics Letters*, 2011, 98: 141913.
- [12] GAO X Q, ZHAO K, KE H B, et al. High mixing entropy bulk metallic glasses [J]. *Journal of Non-Crystalline Solids*, 2011, 357: 3557–3560.
- [13] TAKEUCHI A, CHEN N, WADA T, et al. Pd<sub>20</sub>Pt<sub>20</sub>Cu<sub>20</sub>Ni<sub>20</sub>P<sub>20</sub> high-entropy alloy as a bulk metallic glass in the centimeter [J]. *Intermetallics*, 2011, 19: 1546–1554.
- [14] WANG W H. Roles of minor additions in formation and properties of bulk metallic glasses [J]. *Progress in Materials Science*, 2007, 52: 540–596.
- [15] LIU C T, CHISHOLM M F, MILLER M K. Oxygen impurity and microalloying effect in a Zr-based bulk metallic glass alloy [J]. *Intermetallics*, 2002, 10: 1105–1112.
- [16] LU Z P, LIU C T. Role of minor alloying additions in formation of bulk metallic glasses: A review [J]. *Journal of Materials Science*, 2004, 39: 3965–3974.
- [17] LIU C T, LU Z P. Effect of minor alloying additions on glass formation in bulk metallic glasses [J]. *Intermetallics*, 2005, 13: 415–418.

- [18] ZHANG T, LI R, PANG S J. Effect of similar elements on improving glass-forming ability of La-Ce-based alloys [J]. *Journal of Alloys and Compounds*, 2009, 483: 60–63.
- [19] LI R, LIU F J, PANG S, et al. The influence of similar element coexistence in (La-Ce)-Al-(Co-Cu) bulk metallic glasses [J]. *Materials Transactions*, 2007, 48: 1680–1683.
- [20] GUO S, NG C, LU J, et al. Effect of valence electron concentration on stability of fcc or bcc phase in high entropy alloys [J]. *Journal of Applied Physics*, 2011, 109: 103505.
- [21] CAHN R W, HASSEN P. *Physical Metallurgy* [M]. 4th Ed. Vol.1. Amsterdam: North Holland, 1996.
- [22] TONG C J, CHEN Y L, CHEN S K, et al. Microstructure characterization of Al<sub>x</sub>CoCrCuFeNi high-entropy alloy system with multiprincipal elements [J]. *Metallurgical and Materials Transactions A*, 2005, 36: 881–893.
- [23] ZHANG Y, ZHOU Y J, LIN J P, et al. Solid-solution phase formation rules for multi-component alloys [J]. *Advanced Engineering Materials*, 2008, 10: 534–538.
- [24] FANG S S, XIAO X, LEI X, et al. Relationship between the widths of supercooled liquid regions and bond parameters of Mg-based bulk metallic glasses [J]. *Journal of Non-Crystalline Solids*, 2003, 321: 120–125.
- [25] LIU C T. Physical metallurgy and mechanical properties of ductile ordered alloys (Fe, Co, Ni)<sub>3</sub>V [J]. *International Metals Reviews*, 1984, 29: 168–194.
- [26] ZHU J H, LIAW P K, LIU C T. Effect of electron concentration on the phase stability of NbCr<sub>2</sub>-based Laves phase alloys [J]. *Materials Science and Engineering A*, 1997, 239–240: 260–264.
- [27] MIZUTANI U. Hume-Rothery rules for structurally complex alloy phases [M]. Boca Raton: CRC Press, 2011.
- [28] MASSALSKI T B. Comments concerning some features of phase diagrams and phase transformations [J]. *Materials Transactions*, 2010, 51: 583–596.
- [29] TAKEUCHI A, INOUE A. Calculations of mixing enthalpy and mismatch entropy for ternary amorphous alloys [J]. *Materials Transactions*, 2000, 41: 1372–1378.
- [30] TAKEUCHI A, INOUE A. Classification of bulk metallic glasses by atomic size difference, heat of mixing and period of constituent elements and its application to characterization of the main alloying element [J]. *Materials Transactions*, 2005, 46: 2817–2829.
- [31] WEN L H, KOU H C, LI J S, et al. Effect of aging temperature on microstructure and properties of AlCoCrCuFeNi high-entropy alloy [J]. *Intermetallics*, 2009, 17: 266–269.
- [32] LIN C M, TSAI H L, BOR H Y. Effect of aging treatment on microstructure and properties of high-entropy Cu<sub>0.5</sub>CoCrFeNi alloy [J]. *Intermetallics*, 2010, 18: 1244–1250.
- [33] LIN C M, TSAI H L. Equilibrium phase of high-entropy FeCoNiCrCu<sub>0.5</sub> alloy at elevated temperature [J]. *Journal of Alloys and Compounds*, 2010, 489: 30–35.
- [34] SENKOV O N, WILKS G B, SCOTT J M, et al. Mechanical properties of Nb<sub>25</sub>Mo<sub>25</sub>Ta<sub>25</sub>W<sub>25</sub> and V<sub>20</sub>Nb<sub>20</sub>Mo<sub>20</sub>Ta<sub>20</sub>W<sub>20</sub> refractory high entropy alloys [J]. *Intermetallics*, 2011, 19: 698–706.
- [35] LAI C H, LIN S J, YEH J W, et al. Effect of substrate bias on the structure and properties of multi-element (AlCrTaTiZr)<sub>N</sub> coatings [J]. *Journal of Physics D: Applied Physics*, 2006, 39: 4628–4633.
- [36] COHEN M H, TURNBULL D. Composition requirements for glass formation in metallic and ionic systems [J]. *Nature*, 1961, 189: 131–132.
- [37] CANTOR B, CAHN R W. Metastable alloy phases by co-sputtering [J]. *Acta Metallurgica*, 1976, 24: 845–852.
- [38] LI Y, POON S J, SHIFLET G J, et al. Formation of bulk metallic glasses and their composites [J]. *MRS Bulletin*, 2007, 32: 624–628.
- [39] GREER A L. Confusion by design [J]. *Nature*, 1993, 366: 303–304.
- [40] EGAMI T, WASEDA Y. Atomic size effect on the formability of metallic glasses [J]. *Journal of Non-Crystalline Solids*, 1984, 64: 113–134.
- [41] EGAMI T. Universal criterion for metallic glass formation [J]. *Materials Science and Engineering A*, 1997, 226: 261–267.
- [42] EGAMI T. Atomic level stresses [J]. *Progress in Materials Science*, 2011, 56: 637–653.
- [43] PARK J M, NA J H, KIM D H, et al. Medium range ordering and its effect on plasticity of Fe-Mn-B-Y-Nb bulk metallic glass [J]. *Philosophical Magazine*, 2010, 90: 2619–2633.
- [44] MATTERN N. Structure formation in liquid and amorphous metallic alloys [J]. *Journal of Non-Crystalline Solids*, 2007, 353: 1723–1731.
- [45] FUJITA T, KONNO K, ZHANG W, et al. Atomic-scale heterogeneity of a multicomponent bulk metallic glass with excellent glass forming ability [J]. *Physical Review Letters*, 2009, 103: 075502.
- [46] <http://www.webelements.com/>.
- [47] SENKOV O N, MIRACLE D B. Effect of the atomic size distribution on glass forming ability of amorphous metallic alloys [J]. *Materials Research Bulletin*, 2001, 36: 2183–2198.
- [48] CHEN Y Y, DUVAL T, HONG U T, et al. Corrosion properties of a novel bulk Cu<sub>0.5</sub>NiAlCoCrFeSi glassy alloy in 288 °C high-purity water [J]. *Materials Letters*, 2007, 61: 2692–2696.
- [49] YANG T H, HUANG R T, WU C A, et al. Effect of annealing on atomic ordering of amorphous ZrTaTiNbSi alloy [J]. *Applied Physics Letters*, 2009, 95: 241905.
- [50] TANG M B, ZHAO D Q, PAN M X, et al. Binary Cu-Zr bulk metallic glasses [J]. *Chinese Physics Letters*, 2004, 21: 901–903.
- [51] REINEKE E G, INAL O T. Crystallization behavior of amorphous Ni<sub>50</sub>Nb<sub>50</sub> on continuous heating [J]. *Materials Science and Engineering*, 1983, 57: 223–231.
- [52] PLUMMER J D, CUNLIFFE A J, FIGUEROA A I, et al. Glass formation in a high entropy alloy [C]/Presentation at the 8th International Conference on Bulk Metallic Glasses. Hong Kong, 2011.
- [53] HSIEH P J, LO Y C, WANG C T, et al. Cyclic transformation between nanocrystalline and amorphous phases in Zr based intermetallic alloys during ARB [J]. *Intermetallics*, 2007, 15: 644–651.
- [54] HU C J, WU H M, CHEN T Y. Synthesis of Mg-Cu-Ti based amorphous alloys by mechanical alloying technique [J]. *Journal of Physics: Conference Series*, 2009, 144: 012020.
- [55] AYDINBEYLI N, CELIK O N, GASAN H, et al. Effect of the heating rate on crystallization behavior of mechanically alloyed Mg<sub>50</sub>Ni<sub>50</sub> amorphous alloy [J]. *International Journal of Hydrogen Energy*, 2006, 31: 2266–2273.
- [56] MA L Q, WANG L M, ZHANG T, et al. Bulk glass formation of Ti-Zr-Hf-Cu-M (M=Fe, Co, Ni) alloys [J]. *Materials Transactions*, 2002, 43: 277–280.
- [57] CHANG H W, HUANG P K, DAVISON A, et al. Nitride films deposited from an equimolar Al-Cr-Mo-Si-Ti alloy target by reactive direct current magnetron sputtering [J]. *Thin Solid Films*, 2008, 516: 6402–6408.
- [58] CHENG K H, LAI C H, LIN S J, et al. Structural and mechanical properties of multi-element (AlCrMoTaTiZr)<sub>N<sub>x</sub></sub> coatings by reactive magnetron sputtering [J]. *Thin Solid Films*, 2011, 519: 3185–3190.

- [59] TSAI M H, YEH J W, GAN J Y. Diffusion barrier properties of AlMoNbSiTaTiVZr high-entropy alloy layer between copper and silicon [J]. Thin Solid Films, 2008, 516: 5527–5530.
- [60] ZHANG H, PAN Y, HE Y Z, et al. Microstructure and properties of 6FeNiCoSiCrAlTi high-entropy alloy coating prepared by laser cladding [J]. Applied Surface Science, 2011, 257: 2259–2263.
- [61] SENKOV O N, WILKS G B, MIRACLE D B, et al. Refractory high-entropy alloys [J]. Intermetallics, 2010, 18: 1758–1765.
- [62] TUNG C C, YEH J W, SHUN T T, et al. On the elemental effect of AlCoCrCuFeNi high-entropy alloy system [J]. Materials Letters, 2007, 61: 1–5.
- [63] KE G Y, CHEN S K, HSU T, et al. FCC and BCC equivalents in as-cast solid solutions of  $\text{Al}_x\text{Co}_y\text{Cr}_z\text{Cu}_{0.5}\text{Fe}_v\text{Ni}_w$  high-entropy alloys [J]. Annales De Chimie-Science Des Materiaux, 2006, 31: 669–683.
- [64] CHEN H Y, TSAI C W, TUNG C C, et al. Effect of the substitution of Co by Mn in Al–Cr–Cu–Fe–Co–Ni high-entropy alloys [J]. Annales De Chimie-Science Des Materiaux, 2006, 31: 685–698.
- [65] YEH J W, CHANG S Y, HONG Y D, et al. Anomalous decrease in X-ray diffraction intensities of Cu–Ni–Al–Co–Cr–Fe–Si alloy systems with multi-principal elements [J]. Materials Chemistry and Physics, 2007, 103: 41–46.
- [66] CHIANG C W. Microstructure and properties of as-cast 10-component nanostructured AlCoCrCuFeMoNiTiVZr high-entropy alloy [D]. Taiwan: National Tsinghua University, 2004.
- [67] ZHOU Y J, ZHANG Y, WANG Y L, et al. Microstructure and compressive properties of multicomponent  $\text{Al}_x(\text{TiVCrMnFeCo-NiCu})_{100-x}$  high-entropy alloys [J]. Materials Science and Engineering A, 2007, 454–455: 260–265.
- [68] WANG X F, ZHANG Y, QIAO Y, et al. Novel microstructure and properties of multicomponent CoCrCuFeNiTi<sub>x</sub> alloys [J]. Intermetallics, 2007, 15: 357–362.
- [69] CHEN M R, LIN S J, YEH J W, et al. Microstructure and properties of  $\text{Al}_{0.5}\text{CoCrCuFeNiTi}_x$  ( $x=0\text{--}2.0$ ) high-entropy alloys [J]. Materials Transactions, 2006, 47: 1395–1401.
- [70] CHEN M R, LIN S J, YEH J W, et al. Effect of vanadium addition on the microstructure, hardness, and wear resistance of  $\text{Al}_{0.5}\text{CoCrCuFeNi}$  high-entropy alloy [J]. Metallurgical and Materials Transactions A, 2006, 37: 1363–1369.
- [71] YANG J Y, ZHOU Y J, ZHANG Y, et al. Solid solution formation criteria in the multi-component alloys with high entropy of mixing [J]. Chinese Materials Science Technology & Equipment, 2007, 5: 61–63.
- [72] ZHOU Y J, ZHANG Y, WANG Y L, et al. Solid solution alloys of AlCoCrFeNiTi<sub>x</sub> with excellent room-temperature mechanical properties [J]. Applied Physics Letters, 2007, 90: 181904.
- [73] GUO S, LIU C T. New glass forming ability criterion derived from cooling consideration [J]. Intermetallics, 2010, 18: 2065–2068.